Efficient Contrast Enhancement Using Adaptive Gamma Correction With Weighting Distribution

Shih-Chia Huang, Fan-Chieh Cheng, and Yi-Sheng Chiu

***Abstract*— This paper proposes an efficient method to modify histograms and enhance contrast in digital images. Enhancement plays a significant role in digital image processing, computer vision, and pattern recognition. We present an automatic transformation technique that improves the brightness of dimmed images via the gamma correction and probability distribution of luminance pixels. To enhance video, the proposed image-enhancement method uses temporal information regarding the differences between each frame to reduce computational complexity. Experimental results demonstrate that the proposed method produces enhanced images of comparable or higher quality than those produced using previous state-of-the-art methods.**

***Index Terms*— Contrast enhancement, gamma correction, histogram equalization, histogram modification.**

I. Introduction

CONTRAST enhancement plays an important role in the improvement of visual quality for computer vision, pattern recognition, and the processing of digital images. Poor contrast in digital video or images can result from many circumstances, including lack of operator expertise and inadequacy of the image capture device. Unfavorable environmental conditions in the captured scene, such as the presence of clouds, lack of sunlight or indoor lighting, and other conditions, might also lead to reduced contrast quality [1]. Essentially, if the overall luminance is insufficient, then the details of the image or video features will be obscured.

In general, the enhancement techniques for dimmed images can be broadly divided into two categories: direct enhancement methods [2]–[4] and indirect enhancement methods [5]–[7]. In direct enhancement methods, the image contrast can be directly defined by a specific contrast term [2]–[4]. However, most of these metrics cannot simultaneously gauge the contrast of simple and complex patterns in images which contain both [4].

Conversely, indirect enhancement methods attempt to enhance image contrast by redistributing the probability density [1]. In other words, the image intensities can be redistributed within the dynamic range without defining a specific contrast term [1]. Histogram modifications (HM) techniques [8]–[18] are the most popular indirect enhancement techniques due to their easy and fast implementation [1].

Gamma correction techniques make up a family of general HM techniques obtained simply by using a varying adaptive parameter γ. The simple form of the transform-based gamma correction (TGC) is derived by

$$T(l) = l_{\max}(l/l_{\max})^{\gamma} \tag{1}$$

where $l_{\max}$ is the maximum intensity of the input. The intensity l of each pixel in the input image is transformed as $T(l)$ after performing Eq. (1). As expected, the gamma curves illustrated with $\gamma > 1$ have exactly the opposite effect as those generated with $\gamma < 1$, as shown in Fig. 1(a). It is important to note that gamma correction reduces toward the identity curve when $\gamma = 1$.

However, when the contrast is directly modified by gamma correction, different images will exhibit the same changes in intensity as a result of the fixed parameter. Fortunately, the probability density of each intensity level in a digital image can be calculated to solve this problem. The probability density function (pdf) can be approximated by

$$pdf(l) = n_l/(MN) \tag{2}$$

where n_l is the number of pixels that have intensity l and MN is the total number of pixels in the image. The cumulative distribution function (cdf) is based on pdf, and is formulated as:

$$cdf(l) = \sum_{k=0}^{l} pdf(k). \tag{3}$$

After the cdf of the digital image is obtained from Eq. (3), traditional Histogram Equalization (THE) directly uses cdf as a transformation curve expressed by

$$T(l) = cdf(l)l_{\max}. \tag{4}$$

Fig. 1(b) shows an example of the transformation curve of THE. It is important to note that the transformation of the THE method degrades toward the identity line when pdf is the most uniform with maximum entropy.

Various disadvantages exist in regard to the TGC and THE methods. Fig. 1(c) and (d) show the modified values of each intensity by using the corresponding curves illustrated in Fig. 1(a) and (b). The x-coordinate is the input intensity and the y-coordinate is the decrement or increment of each intensity level. As shown in Fig. 1(c), unvaried modification

Manuscript received January 29, 2012; revised June 12, 2012; accepted October 07, 2012. Date of publication October 22, 2012; date of current version January 24, 2013. This work was supported in part by the National Science Council under Grant NSC 100-2628-E-027-012-MY3. The associate editor coordinating the review of this manuscript and approving it for publication was Dr. Debargha Mukherjee.

The authors are with the Department of Electronic Engineering, National Taipei University of Technology, Taipei 106, Taiwan (e-mail: schuang@ntut.edu.tw; d9802108@mail.ntust.edu.tw; t8418012@ntut.edu.tw).

Color versions of one or more of the figures in this paper are available online at http://ieeexplore.ieee.org.

Digital Object Identifier 10.1109/TIP.2012.2226047

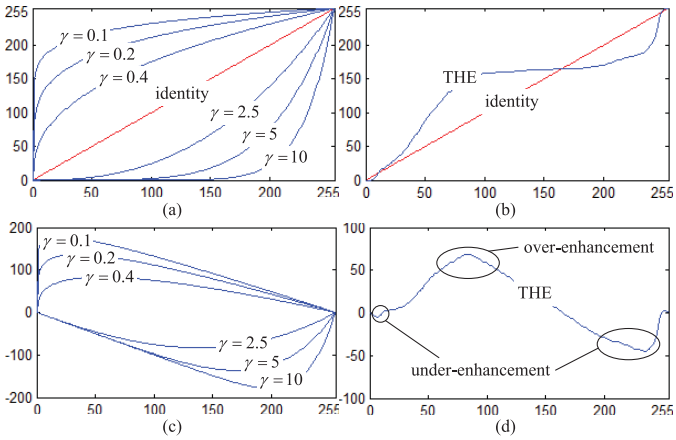

Fig. 1. Transformation curves illustrated by (a) gamma correction and (b) THE methods, with their corresponding intensity level modifications shown in (c) and (d).

is produced by the use of the TGC method with a predefined parameter. On the other hand, the THE method uses the property of the histogram to enhance the intensity contrast; this inappropriate modification is shown in Fig. 1(d). Over-enhancement and under-enhancement are indeed major challenges due to the unnatural changes in cdf. For example, three areas are circled in Fig. 1(d) that point out these adverse effects: some low intensity levels are still decreased, moderate intensity levels are significantly increased, and high intensity levels are significantly decreased.

The rest of this paper is organized as follows: Section II provides a brief discussion of related works. Section III presents our proposed method in detail. In Section IV, the efficacy of the proposed method is supported by comparing the experimental results obtained through use of our method to those obtained via existing methods. Finally, our concluding remarks are presented in Section V.

II. Previous Works

In order to solve the aforementioned problems associated with the THE method, earlier works individually equalized two sub-histograms produced by separation techniques [8], [9]. The Brightness-preserving Bi-Histogram Equalization (BBHE) method calculates the mean intensity as the threshold value [8], while the Dualistic Sub-Image Histogram Equalization (DSIHE) method uses the median instead of the mean [9]. The Brightness-Preserving Histogram Equalization with Maximum Entropy (BPHEME) method preserves the brightness and also maximizes the entropy of the enhanced image via histogram speciation [10]. After segmentation overlaps the sub-blocks of the image, the THE method should be employed several times to enhance the local contrast per block. To reduce the computational cost, Cascaded Multistep Binomial Filtering Histogram Equalization (CMBFHE) was utilized in order to achieve the same low-pass filter mask [11]. However, its time complexity is still much higher than BBHE and DSIHE.

The Recursive Sub-Image Histogram Equalization (RSIHE) method features the same time complexity, but extends DSIHE by including multi-equalizations to reduce the generation of artifacts [12]. However, this problem cannot be effectively solved by using its recursive nature and scalable brightness preservation techniques. In addition to histogram separation techniques, the Recursively Separated and Weighted Histogram Equalization (RSWHE) method uses a weighting function to smooth each sub-histogram for image enhancement as well as brightness preservation [13]. As the original histogram is subject to the brightness constraint, the Flattest Histogram Specification with Accurate Brightness Preservation (FHSABP) method utilizes convex optimization [14]. In order to concurrently apply TGC and THE, the Dynamic Contrast Ratio Gamma Correction (DCRGC) method directly sets a parameter as a ratio. However, it cannot be automatically generated [15].

Contrast enhancement can be optimized by the histogram modification framework (HMF), which incorporates penalty terms for histogram deviation as well as minimizes a cost function to compute a target histogram [1]. In order to accurately preserve brightness, the Automatic Weighting Mean-separated Histogram Equalization (AWMHE) method uses the recursive function to optimize the threshold values applied to equalize sub-histograms [16]. The aforementioned techniques use only a one-dimensional (1-D) histogram, even if it might possess spikes which compress other gray-levels for distribution. To alleviate the previously discussed problem, the two-dimensional (2-D) histogram is used to generate contextual and variational information in the image [17], while the Gaussian Mixture Model (GMM) can also be used to compensate for the gray-level distribution of the image [18]. The Contextual and Variational Contrast (CVC) enhancement method is more effective at showing the visual quality of the image, because it directly constructs an a priori probability, which further represents details of the image [17]. However, the CVC method requires a high level of computation when increasing the gray-level differences between neighboring pixels.

III. Proposed Method

To compensate for the limitations of these methods, a technique must be developed which creates a balance between high levels of visual quality and low computational costs. In this paper, a hybrid HM method is proposed to accomplish this goal by efficiently combining the TGC and THE methods. As indicated in the description of the RSWHE method, a normalized gamma function can be used to modify each sub-histogram to include multi-equalizations with brightness preservation [13]. However, the modified sub-histograms might lose some statistical information, thus reducing the effect of enhancement. Inspired by the RSWHE method [13], we directly utilized cdf and applied a normalized gamma function to modify the transformation curve without losing the available histogram of statistics. Consequently, the lower gamma parameter generates a more significant adjustment. This observation led us to employ a compensated cdf as an adaptive parameter, which modifies the intensity with a progressive increment of the original trend. The proposed adaptive gamma correction (AGC) is formulated as follows:

$$T(l) = l_{\max}(l/l_{\max})^{\gamma} = l_{\max}(l/l_{\max})^{1-cdf(l)}. \quad (5)$$

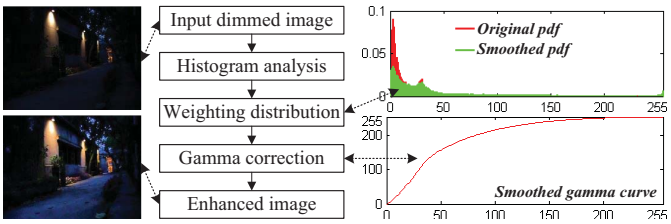

Fig. 2. Flowchart of the AGCWD method.

The AGC method can progressively increase the low intensity and avoid the significant decrement of the high intensity.

Furthermore, the weighting distribution (WD) function is also applied to slightly modify the statistical histogram and lessen the generation of adverse effects [13]. The WD function is formulated as:

$$pdf_w(l) = pdf_{\max}\left(\frac{pdf(l) - pdf_{\min}}{pdf_{\max} - pdf_{\min}}\right)^{\alpha} \tag{6}$$

where α is the adjusted parameter, $pdf_{\max}$ is the maximum pdf of the statistical histogram, and $pdf_{\min}$ is the minimum pdf. Based on Equation (6), the modified cdf is approximated by

$$cdf_w(l) = \sum_{l=0}^{l_{\max}} pdf_w(l) / \Sigma pdf_w \tag{7}$$

where the sum of pdf_w is calculated as follows:

$$\Sigma pdf_w = \sum_{l=0}^{l_{\max}} pdf_w(l). \tag{8}$$

Finally, the gamma parameter based on cdf of Equation (5) is modified as follows:

$$\gamma = 1 - cdf_w(l). \tag{9}$$

According to studies [19] and [20], color images can be enhanced to be acceptable to human vision by using the HSV color model, which can decouple the achromatic and chromatic information of the original image in order to maintain color distribution. In the HSV color model, the hue (H) and the saturation (S) can be used to represent the color content, with the value (V) representing the luminance intensity. The color image can be enhanced by preserving H and S while enhancing only V. Hence, the proposed AGC with WD (AGCWD) method was applied to the V component for color-contrast enhancement.

Fig. 2 shows the flowchart of the proposed AGCWD method. For the dimmed image used as input, most of the pixels are densely distributed in the low-level region. Based on the weighting distribution function, the fluctuant phenomenon can be smoothed, thus reducing the over-enhancement of the gamma correction. To the best of our knowledge, we are the first researchers to feature a combination of cdf, weighting distribution, and gamma correction. Our proposed AGCWD method can enhance a color image without generating artifacts or distorting the color.

In addition to image-contrast enhancement, we also propose a temporal-based (TB) technique to further reduce the computational complexity required by the AGCWD method to enhance a video sequence. Fig. 3 shows the flowchart of the TB method as applied for video-contrast enhancement.

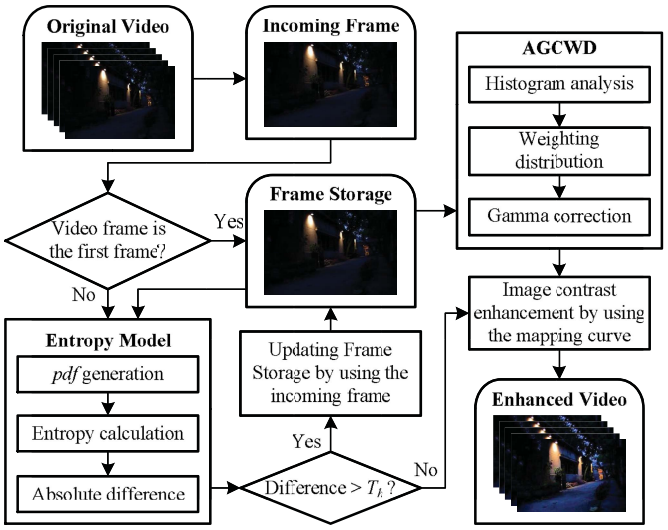

Fig. 3. Flowchart of the TB method applied to a video sequence.

At the beginning of the process, the first incoming frame is directly stored in the frame storage, which is used to generate a mapping curve for the proposed AGCWD method. For subsequent incoming video frames, the entropy model can be used to measure the differences of the information content between two successive frames. The information content of each frame is approximated by the following entropy formula:

$$H = -\sum_{l=0}^{l_{\max}} pdf(l)\log(pdf(l)). \tag{10}$$

When the absolute difference between the current H and previous H exceeds threshold T_h, the frame storage can be updated by the incoming frame, while the transformation curve is also modified. In this situation, T_h is empirically set to 0.05. Otherwise, the existing mapping curve is directly applied to transform each intensity level in the incoming video frame.

IV. Experimental Results

This section summarizes the experimental results produced by nine HM and HM-based methods, including THE, BBHE [8], DSIHE [9], RSIHE [12], RSWHE [13], DCRGC [15], AWMHE [16], and CVC [17], along with our proposed AGCWD method. For image-contrast enhancement, these methods were applied to enhance various grayscale and color images. This paper follows the same decomposition of the histogram used by other researchers [12], [13], and includes four sub-histograms. The gamma parameter of DCRGC can be set to 2.2 with the adaptive factor equal to 0.75 [15]. To facilitate searching neighborhoods via the CVC method, the radius has been fixed to 3 [17].

In general, illumination changes can be caused by many factors common to outdoor scenes, such as the intensity of the sunshine, the location of the light source, cloud cover, and many others. For images of indoor scenes, the quality is often

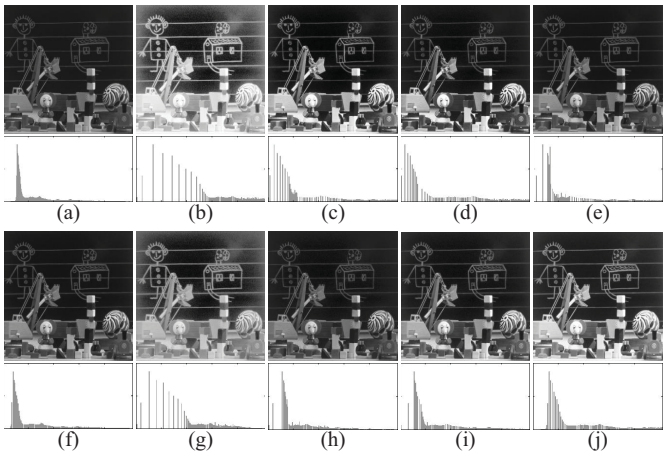

Fig. 4. *Blackboard* image. (a) Original image with its corresponding statistical histogram; the remaining nine images are the enhancement results with modified histograms generated by the (b) THE, (c) BBHE, (d) DSIHE, (e) RSIHE, (f) RSWHE, (g) DCRGC, (h) AWMHE, (i) CVC, and (j) AGCWD methods.

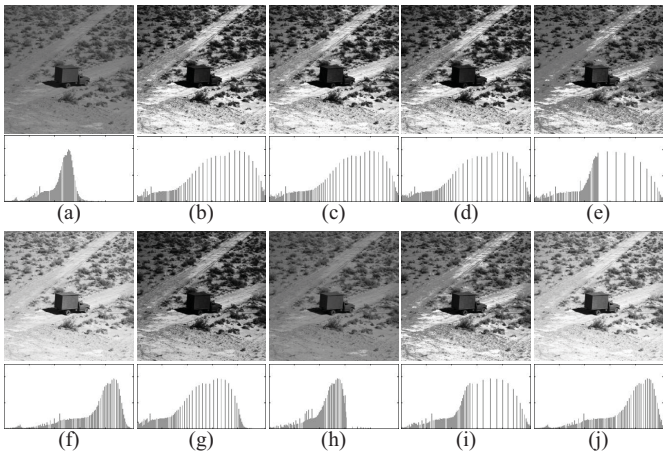

Fig. 5. *Truck* image. (a) Original image with its corresponding statistical histogram; the remaining nine images are the enhancement results with modified histograms generated by the (b) THE, (c) BBHE, (d) DSIHE, (e) RSIHE, (f) RSWHE, (g) DCRGC, (h) AWMHE, (i) CVC, and (j) AGCWD methods.

affected by interior lighting. Therefore, we used several images captured from both outdoor and indoor scenes to evaluate each method.

A. Visual Assessment

Contrast enhancement, performed by each method, was initially measured by a visual assessment of four grayscale images named *Blackboard*, *truck*, *viaduct*, and *warplane*. Fig. 4 shows the *Blackboard* image and enhancement results using statistical histograms generated by each method. The original picture displayed in Fig. 4(a) includes a blackboard and many playthings in a classroom. The THE method directly equalized the original histogram of the original picture, thus losing some information of intensity, as indicated in Fig. 4(b). As shown in Fig. 4(c) and (d), both the BBHE and DSIHE methods separately equalized the low level and high level of the histogram to solve the problem produced by the THE method. However, the luminance could not be improved by the two bi-equalizations. The RSIHE method used multi-equalizations extended from the DSIHE method to enhance the contrast. Unfortunately, the improved luminance was not uniform, as displayed in Fig. 4(e). The RSWHE method slightly equalized the original picture to preserve brightness via the use of modified information from the original histogram, but the contrast of the enhanced image, shown in Fig. 4(f), was not adequately improved. As shown in Fig. 4(g), the DCRGC method directly averaged the transformation curves generated by the TGC and THE methods to enhance the image, thus reducing the problem that exists for the THE method. The AWMHE method automatically generated sub-histograms and specifically equalized them to preserve the brightness, as shown in Fig. 4(h). The enhanced contrast is slight and similar to the RSWHE method. The CVC method searched neighborhoods of pixels in order to generate the contextual 2-D histogram, which was applied for HM optimization, as shown in Fig. 4(i). The proposed AGCWD method automatically calculated the gamma parameter via probability density to combine the TGC and THE methods efficiently. As shown in Fig. 4(j), the resultant modified histogram is more uniform than that generated by the DCRGC method.

Fig. 5 shows the *truck* image and enhancement results with statistical histograms produced by the THE, BBHE, DSIHE, RSIHE, RSWHE, DCRGC, AWMHE, CVC, and AGCWD methods. The original picture shown in Fig. 5(a) contains a truck moving on the ground on which a sparse amount of plants are growing. As shown in Fig. 5(b), the THE method produced an image with unnatural contrast due to the non-uniform histogram. Because most of the gray-levels are smaller than the mean and median, a good contrast image could not be produced by either the BBHE method or the DSIHE method, as indicated in Fig. 5(c) and (d). It is important to note that the low-level histogram shows a large equalization of the probability. Therefore, similar results were produced to make the effects of the THE method more appropriate. The RSIHE method improved the DSIHE method by including multi-equalizations. Unfortunately, most of the resultant sub-histograms were distributed over the low-level of the original histograms. Therefore, the high level of the original image and histogram could not be enhanced well, as shown in Fig. 5(e). The RSWHE method employed a weighted function to avoid the generation of artifacts. Subsequently, the resultant image exhibits acceptable quality, as shown in Fig. 5(f). The DCRGC method has the ability to reduce the adverse effects of the THE method, while the illustrated curve was employed for reference by the TGC method. However, as Fig. 5(g) shows, a low-quality image with unnatural contrast was still generated. The AWMHE method severely segmented the histogram in order to preserve the original content, as shown in Fig. 5(h). As displayed in Fig. 5(i), the CVC method extended the 2-D histogram for equalization of the image. However, the high-level histogram continues to be sparse. In contrast to the shortcomings of these other methods, the proposed AGCWD method effectively remedied their

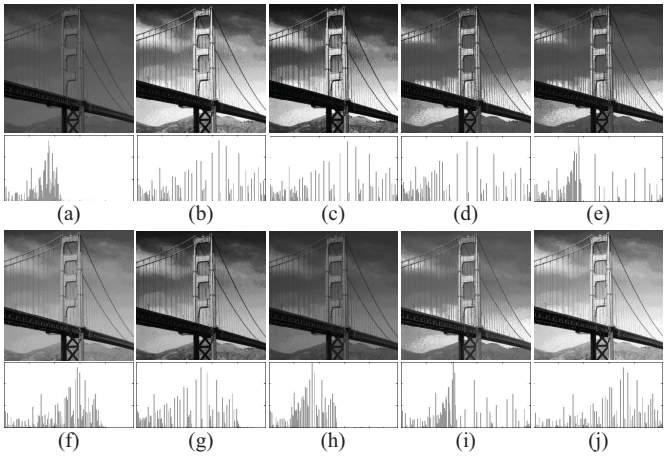

Fig. 6. *Viaduct* image. (a) Original image with its corresponding statistical histogram. The remaining nine images are the enhancement results with modified histograms generated by the (b) THE, (c) BBHE, (d) DSIHE, (e) RSIHE, (f) RSWHE, (g) DCRGC, (h) AWMHE, (i) CVC, and (j) AGCWD methods.

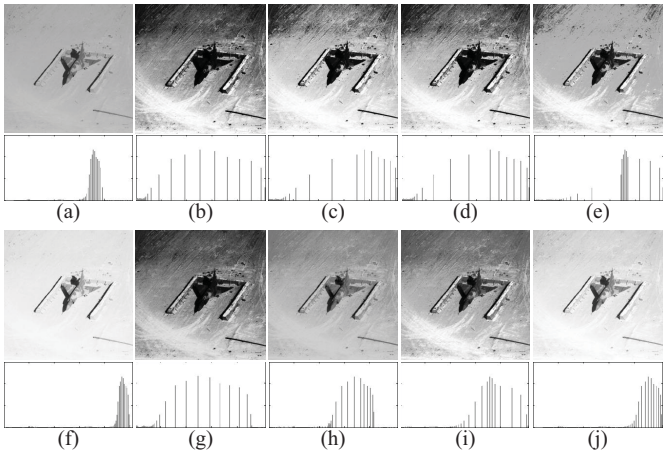

Fig. 7. *Warplane* image. (a) Original image with its corresponding statistical histogram. The remaining nine images are the enhancement results with modified histograms generated by the (b) THE, (c) BBHE, (d) DSIHE, (e) RSIHE, (f) RSWHE, (g) DCRGC, (h) AWMHE, (i) CVC, and (j) AGCWD methods.

problems and produced an image with good contrast, as can be seen in Fig. 5(j).

Fig. 6 shows the *viaduct* image and its enhancement results with statistical histograms produced by each method. The original picture features a viaduct and a background with low contrast, as shown in Fig. 6(a). The THE method directly equalized the histogram again to produce an enhanced image in which the histogram lost some gray-levels, as illustrated in Fig. 6(b). As with the *Truck* image, most of the gray-levels in the *viaduct* image are concentrated in the low-level of intensity. Therefore, the BBHE, DSIHE, and RSIHE methods failed again to enhance the contrast, as displayed in Fig. 6(c)–(e). As shown in Fig. 6(f) and (g), the RSWHE and DCRGC methods generated acceptable enhancement results. The AWMHE method slightly equalized the original histogram, while the overall luminance is not changed, as shown in Fig. 6(h). The CVC and AGCWD methods uniformly enhanced the image. However, the generated histogram in Fig. 6(j) is more uniform than that in Fig. 6(i).

Fig. 7 shows the *warplane* image and its enhancement results with equalized histograms produced by the THE, BBHE, DSIHE, RSIHE, RSWHE, DCRGC, AWMHE, CVC, and AGCWD methods. As with Fig. 5(a) and Fig. 6(a), the *warplane* image exhibits low contrast between the object and the background, while most of the gray-levels are distributed over the high-level of intensity, as shown in Fig. 7(a). Subsequently, the THE, BBHE, DSIHE, and RSIHE methods all failed to adequately contend with the low-contrast image, as can be seen in Fig. 7(b)–(e). Although the DCRGC method referenced a transformation curve illustrated by the TGC method, the cumulative distribution was too sparse to easily modify the histogram, as shown in Fig. 7(g). In this case, the RSWHE, AWMHE, CVC, and AGCWD methods did not distort the original brightness, shown in Fig. 7(f), (h)–(j). Nevertheless, the CVC method can be regarded as having produced the clearest edge, which is especially evident upon scrutiny of the ground.

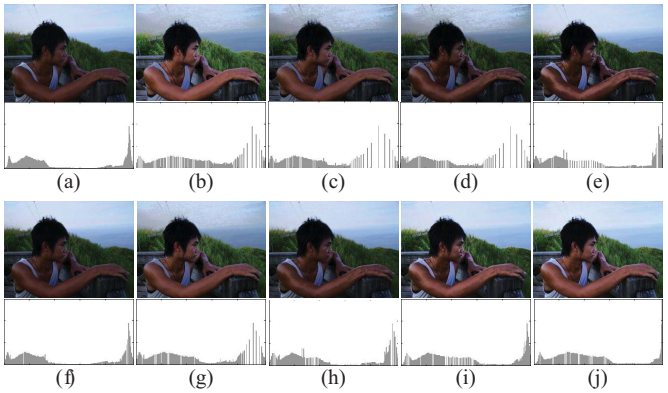

Fig. 8. *Man* image. (a) Original image with its corresponding statistical histogram. The remaining nine images are the enhancement results with modified histograms generated by the (b) THE, (c) BBHE, (d) DSIHE, (e) RSIHE, (f) RSWHE, (g) DCRGC, (h) AWMHE, (i) CVC, and (j) AGCWD methods.

A visual assessment was performed for grayscale images as well as for color images. Fig. 8(a) shows the original *man* image featuring a man relaxing in a gazebo during a day with limited light, while other sub-pictures show enhanced images with equalized histograms generated by each method. Some adverse effects were generated by the THE, BBHE, DSIHE, and RSIHE methods due to non-uniform equalizations. For example, the color of the sky region and the man's skin was distorted after performing these methods, as shown in Fig. 8(b)–(e). Additionally, the RSWHE method did not preserve a sufficient level of the brightness of the original image, thus producing a result with limited contrast, as shown in Fig. 8(f). As demonstrated by Fig. 8(g), the DCRGC method was an improvement on the THE method, but some minor artifacts still exist in the sky region. The AWMHE method modified the brightness in the portion of the image containing skin, yet the contrast was still insufficient, as displayed in Fig. 8(h). The CVC method optimized the contrast, as shown in Fig. 8(i). Unfortunately, the enhanced color appears unnatural when compared to that of the original image.

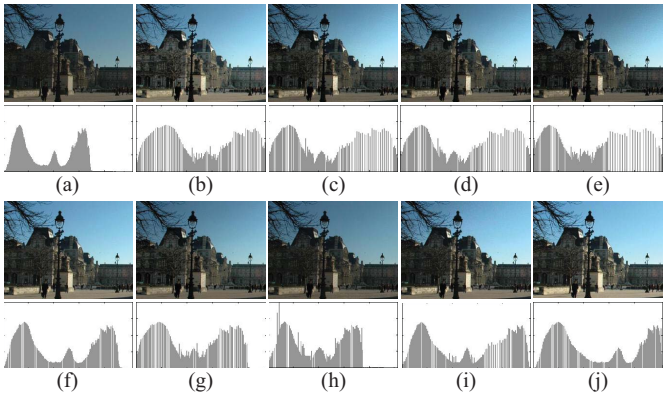

Fig. 9. *Square* image. (a) Original image with its corresponding statistical histogram. The remaining nine images are the enhancement results with modified histograms generated by the (b) THE, (c) BBHE, (d) DSIHE, (e) RSIHE, (f) RSWHE, (g) DCRGC, (h) AWMHE, (i) CVC, and (j) AGCWD methods.

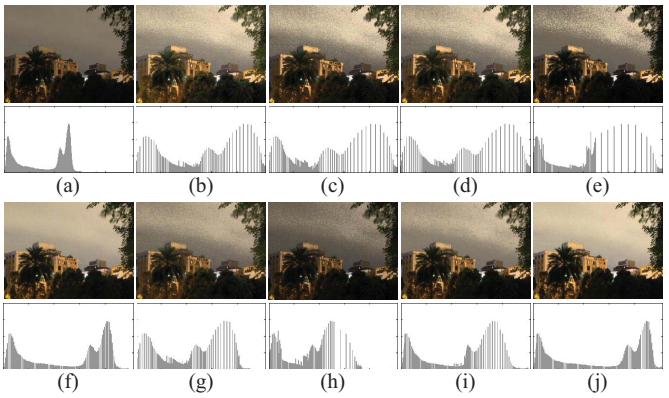

Fig. 10. *Sky* image. (a) Original image with its corresponding statistical histogram. The remaining nine images are the enhancement results with modified histograms generated by the (b) THE, (c) BBHE, (d) DSIHE, (e) RSIHE, (f) RSWHE, (g) DCRGC, (h) AWMHE, (i) CVC, and (j) AGCWD methods.

Fig. 8(j) illustrates that the AGCWD method produced an acceptable image without unnatural or limited contrast.

As shown in Fig. 9(a), the original *square* image includes some buildings, a public square, and an azure sky. For this simple scene, all methods generated acceptable images, as shown in Fig. 9(b)–(j). However, only the AGCWD method produced a uniform improvement of luminance, as shown in Fig. 9(j).

Fig. 10 displays the original *sky* image which was captured at twilight, along with seven enhanced images with equalized histograms generated by each method. Because the high-level intensity of the original image is insufficient, there is not enough information for the THE, BBHE, DSIHE, RSIHE, and DCRGC methods to uniformly equalize the histogram. Therefore, the enhanced images produced by these methods contain serious artifacts in the portions featuring sky. Conversely, both the RSWHE and AGCWD methods improved the luminance, even though the original histogram was not directly applied to generate the transformation function.

Fig. 11 shows the original *road* image, along with its enhancement results produced by the compared methods.

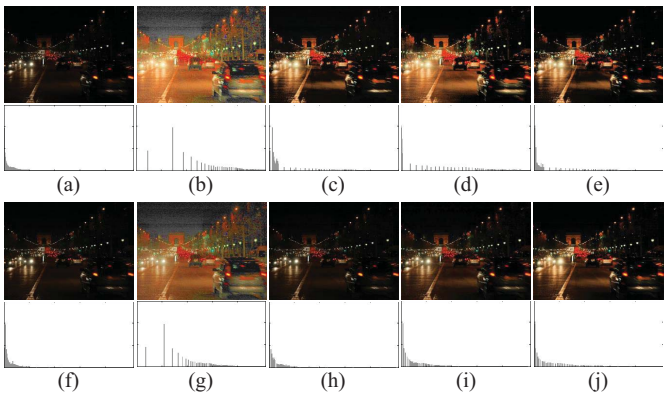

Fig. 11. *Road* image. (a) Original image with its corresponding statistical histogram. The remaining nine images are the enhancement results with modified histograms generated by the (b) THE, (c) BBHE, (d) DSIHE, (e) RSIHE, (f) RSWHE, (g) DCRGC, (h) AWMHE, (i) CVC, and (j) AGCWD methods.

The various HM methods all significantly improved the dark region with the exceptions of RSWHE and AWMHE, which both preserved the low level of brightness as a weak enhancement. It is noteworthy that the CVC and AGCWD methods enhanced the contrast of the image as well as preserving its original features, as shown in Fig. 11(i) and (j).

The subsequent sections will now discuss the performance of all compared methods, which were implemented using the C programming language. In a personal computer with a 3 GHz processor, most HE-based methods required about 0.03 seconds to process one full-HD 1080 p image. The one exception was the CVC method, which required more than four seconds to process the same image due to its exhaustive search of pixel neighborhoods. This discussion provides only a rough comparison of the execution time. The full computational complexity of the procedure depends upon many factors, such as the choice of the hardware platform and the level of software optimization.

B. Quantitative Evaluation

Quantitative evaluation of contrast enhancement is not an easy task, because an acceptable criterion by which to quantify the improved perception has yet to be proposed [1], [17], [18]. In general, objective metrics can be classified as full-reference (FR), no-reference (NR), or reduced-reference methods [21]. Since the efficacy of the known criterion is lost due to the unavailability of a reference image, this paper focuses on the FR method and highlights the use of a "distortion-free" image as the reference image for assessment.

Macbeth ColorChecker is commonly used to analyze images on display devices. ColorChecker is a flat card containing several color blocks with spectral reflectances intended to mimic colors of natural objects such as human skin, foliage, and flowers, while maintaining consistent color appearance under a variety of lighting conditions. ColorChecker requires the preparation of a light box and the use of an illumination meter to assess the environmental values. Therefore, we used a consumer camera, ColorChecker, and an illumination meter to perform the quantitative evaluation in the specific dark room,

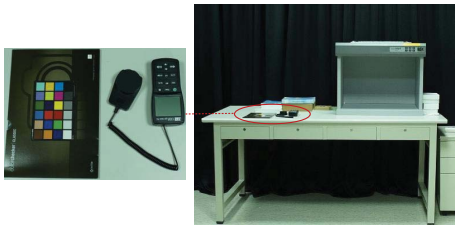

Fig. 12. Snapshots of environments and devices.

TABLE I
STANDARD RGB (sRGB) VALUES OF COLORCHECKER

Block Type	R	G	B
Dark skin	115	82	68
Light skin	194	150	130
Blue sky	98	122	157
Foliage	87	108	67
Blue flower	133	128	177
Bluish green	103	189	170
Orange	214	126	44
Purplish blue	80	91	166
Moderate red	193	90	99
Purple	94	60	108
Yellow green	157	188	64
Orange yellow	224	163	46
Blue	56	61	150
Green	70	148	73
Red	175	54	60
Yellow	231	199	31
Magenta	187	86	149
Cyan	8	133	161
White (.05*)	243	242	242
Neutral 8 (.23*)	200	200	200
Neutral 6.5 (.44*)	160	160	160
Neutral 5 (.70*)	122	122	121
Neutral 3.5 (1.05*)	85	85	85
Black (1.50*)	52	52	52

which are shown in Fig. 12. There are 24 different color blocks in ColorChecker and Table I lists the corresponding color information. From the results, we can easily compare the difference between the target image and the "distortion-free" image; this difference can be used as the objective measurement.

For this paper we analyzed the achromatic and chromatic accuracy of the enhanced image. For the brightness preservation, the modified Absolute Mean Brightness Error (AMBE) was employed to assess the intensity of the enhanced image. The modified AMBE did not measure the difference between the enhanced image and the original image with degraded brightness. The second term is replaced by the sRGB information in Table I. Additionally, the traditional metric ΔE94 which is based on CIE94 was also employed to measure color distortion [22].

In our experiments, images of ColorChecker were captured by the camera in low-light conditions (approximately two lux). Fig. 13 shows three captured images and the enhancement

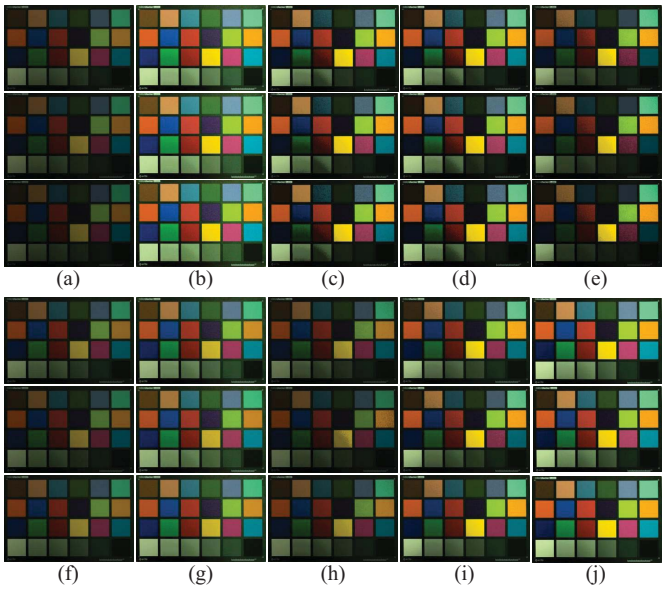

Fig. 13. *ColorChecker* image. (a) Original set of images. The remaining nine sets of images are the enhancement results with modified histograms generated by the (b) THE, (c) BBHE, (d) DSIHE, (e) RSIHE, (f) RSWHE, (g) DCRGC, (h) AWMHE, (i) CVC, and (j) AGCWD methods.

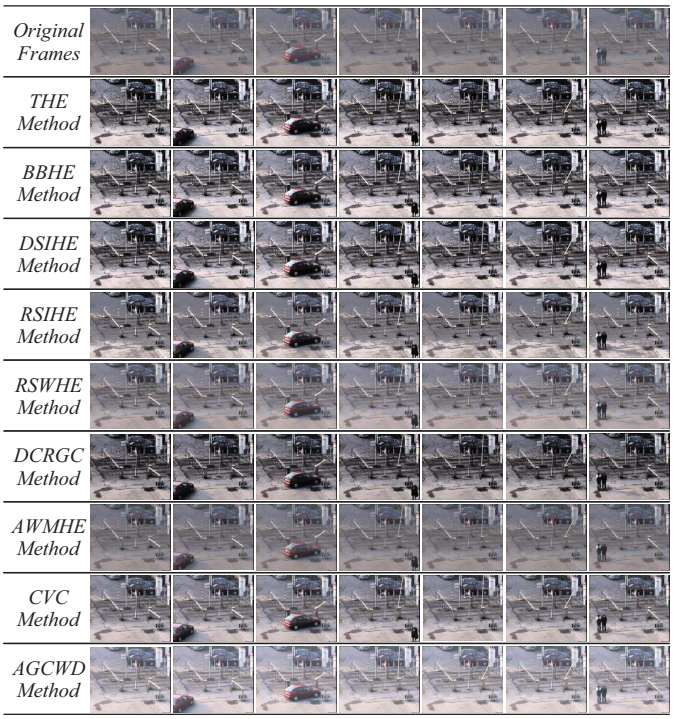

Fig. 14. Seven sampled frames of the *campus* sequence and the enhancement results generated by each method.

results produced by each of the different methods. The images were captured with different exposures (1/3 s, 1/4 s, and 1/5 s) and are displayed from top to bottom. The quantitative evaluations assessed via AMBE and ΔE94 are then listed in Table II and Table III. The results indicate that the proposed method produced enhanced images with the lowest distortion. This is due to an achievement of balance between enhancement of contrast and preservation of image features.

TABLE II
AMBE ASSESSMENT OF CONTRAST ENHANCEMENT METHODS

Exposure Time	THE	BBHE	DSIHE	RSIHE	RSWHE	DCRGC	AWMHE	CVC	AGCWD
1/3 s	9.8	16.5	15.6	25.9	34.1	8.1	34.3	16.6	2.5
1/4 s	9.7	20.4	18.4	30.6	41.0	9.1	41.1	21.1	2.5
1/5 s	9.3	23.5	21.2	34.6	46.6	9.9	47.0	24.7	7.4

TABLE III
ΔE94 ASSESSMENT OF CONTRAST ENHANCEMENT METHODS

Exposure Time	THE	BBHE	DSIHE	RSIHE	RSWHE	DCRGC	AWMHE	CVC	AGCWD
1/3 s	26.0	24.4	23.8	26.3	33.8	26.7	31.2	25.0	23.6
1/4 s	25.7	24.2	23.2	26.6	37.3	26.7	32.9	24.9	22.4
1/5 s	26.2	24.7	23.7	27.6	41.8	27.5	41.4	25.3	22.1

TABLE IV
PERFORMANCE (FPS) EVALUATION FOR THE PROPOSED TB METHOD

Campus Sequence With 600 Frames and 352 × 288 Pixels Per Frame (Statistic Camera)									
Method	THE	BBHE	DSIHE	RSIHE	RSWHE	DCRGC	AWMHE	CVC	AGCWD
Original fps	1190	1172	1181	1167	1158	1165	1152	5	1170
Improved fps	5505	4959	1042	4878	4724	4839	4651	296	4918
Home Sequence With 360 Frames and 480 × 270 Pixels Per Frame (Dynamic Camera)									
Method	THE	BBHE	DSIHE	RSIHE	RSWHE	DCRGC	AWMHE	CVC	AGCWD
Original fps	1198	1190	1187	1179	1169	1172	1162	6	1176
Improved fps	3482	3449	3416	3384	3293	3323	3263	12	3353

C. Enhancement of Video Sequence

In addition to image-contrast enhancement, video-contrast enhancement is also provided for comparison. Fig. 14 shows seven sampled frames of the *campus* color video sequence and its enhancement results generated by each method. In the video, some objects are moving in a dimmed parking area. As indicated by the color of the cars, people, and ground, the THE, BBHE, DSIHE, RSIHE, and DCRGC methods all increased the contrast between the objects and the background. However, some features were seriously distorted. The RSWHE, AWMHE, CVC, and AGCWD methods increased the contrast without distorting color or generating additional artifacts. Ultimately, the AGCWD method generates the clearest luminance while avoiding the distortion of image features.

Fig. 15 shows seven sampled frames of the *home* color video sequence and its enhancement results generated by each method. In the video, a person is shown in an indoor scene under limited lighting conditions. According to the enhancement results, both the THE and DCRGC methods produced very serious luminance and color distortions in the output frames. This is due to the global employment of direct equalization without sufficient information from the histogram. The BBHE, DSIHE, RSIHE, and RSWHE methods reduced the distortions produced by the THE method, but the enhancement results are still unacceptable. Yet again, the proposed AGCWD and TB methods not only increased the contrast but also preserved the image features.

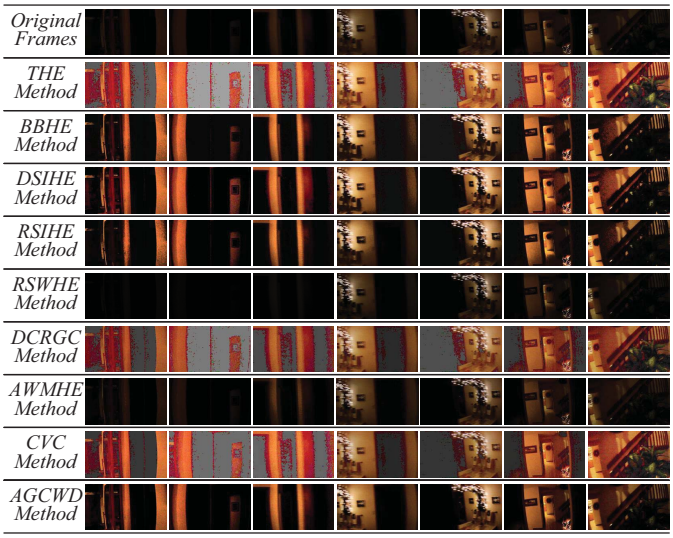

Fig. 15. Seven sampled frames of the *home* sequence and the enhancement results generated by each method.

In order to measure further the differences between the enhanced video generated by the TB method compared and that produced by the AGCWD method, a feature similarity (FSIM) index was used for FR image-quality assessment (IQA) [21]. It is important to note that an FSIM value of 1 represents the highest quality, with 0 representing the lowest quality. Fig. 16 illustrates the FSIM of each frame generated by the AGCWD method with the TB simplification. It is easily

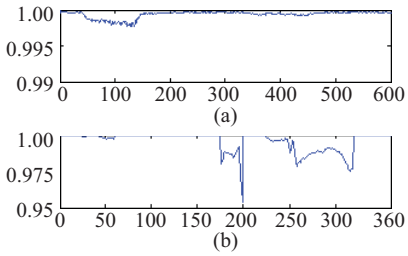

Fig. 16. FSIM of each frame generated by the TB method for (a) *campus* and (b) *home* sequences.

observable that the simplified modification exhibits a small deviation. Furthermore, the TB method can also be applied for other histogram-based methods. Table IV lists the improved rate of frames per second (fps) produced by the proposed TB method for the *campus* and *home* sequences. As a result, the TB method can significantly reduce the processing time, with simplification dependent on the temporal similarity of the sequence.

V. Conclusion

In this paper, we present a novel enhancement method for both images and video sequences. The proposed method is composed of three major steps. First, the histogram analysis provides the spatial information of a single image based on probability and statistical inference. In the second step, the weighting distribution is used to smooth the fluctuant phenomenon and thus avoid generation of unfavorable artifacts. In the third and final step, gamma correction can automatically enhance the image contrast through use of a smoothing curve. Furthermore, we employed temporal information to reduce the computational time for several image frames of a video sequence. Based on the difference of the information content, the entropy model was used to determine whether or not the transformation curve should be updated. Experimental image enhancement results demonstrate that our proposed method performed well compared with other state-of-the-art methods. According to the analysis of time consumption, the proposed method can be implemented in a real-time video system with limited resources.

References

[1] T. Arici, S. Dikbas, and Y. Altunbasak, "A histogram modification framework and its application for image contrast enhancement," *IEEE Trans. Image Process.*, vol. 18, no. 9, pp. 1921–1935, Sep. 2009.

[2] A. Beghdadi and A. L. Negrate, "Contrast enhancement technique based on local detection of edges," *Comput. Vis, Graph., Image Process.*, vol. 46, no. 2, pp. 162–174, May 1989.

[3] H.-D. Cheng and H. J. Xu, "A novel fuzzy logic approach to contrast enhancement," *Pattern Recognit.*, vol. 33, no. 5, pp. 809–819, May 2000.

[4] J. Tang, X. Liu, and Q. Sun, "A direct image contrast enhancement algorithm in the wavelet domain for screening mammograms," *IEEE J. Sel. Topics Signal Process.*, vol. 3, no. 1, pp. 74–80, Feb. 2009.

[5] R. Sherrier and G. Johnson, "Regionally adaptive histogram equalization of the chest," *IEEE Trans. Med. Imag.*, vol. 6, no. 1, pp. 1–7, Jan. 1987.

[6] A. Polesel, G. Ramponi, and V. Mathews, "Image enhancement via adaptive unsharp masking," *IEEE Trans. Image Process.*, vol. 9, no. 3, pp. 505–510, Mar. 2000.

[7] Y.-S. Chiu, F.-C. Cheng, and S.-C. Huang, "Efficient contrast enhancement using adaptive gamma correction and cumulative intensity distribution," in *Proc. IEEE Conf. Syst. Man Cybern.*, Oct. 2011, pp. 2946–2950.

[8] Y. Kim, "Contrast enhancement using brightness preserving bi-histogram equalization," *IEEE Trans. Consum. Electron.*, vol. 43, no. 1, pp. 1–8, Feb. 1997.

[9] Y. Wan, Q. Chen, and B. Zhang, "Image enhancement based on equal area dualistic sub-image histogram equalization method," *IEEE Trans. Consum. Electron.*, vol. 45, no. 1, pp. 68–75, Feb. 1999.

[10] C. Wang and Z. Ye, "Brightness preserving histogram equalization with maximum entropy: A variational perspective," *IEEE Trans. Consum. Electron.*, vol. 51, no. 4, pp. 1326–1334, Nov. 2005.

[11] F. Lamberti, B. Montrucchio, and A. Sanna, "CMBFHE: A novel contrast enhancement technique based on cascaded multistep binomial filtering histogram equalization," *IEEE Trans. Consum. Electron.*, vol. 52, no. 3, pp. 966–974, Aug. 2006.

[12] K. S. Sim, C. P. Tso, and Y. Tan, "Recursive sub-image histogram equalization applied to gray-scale images," *Pattern Recognit. Lett.*, vol. 28, no. 10, pp. 1209–1221, Jul. 2007.

[13] M. Kim and M. G. Chung, "Recursively separated and weighted histogram equalization for brightness preservation and contrast enhancement," *IEEE Trans. Consum. Electron.*, vol. 54, no. 3, pp. 1389–1397, Aug. 2008.

[14] C. Wang, J. Peng, and Z. Ye, "Flattest histogram specification with accurate brightness preservation," *IET Image Process.*, vol. 2, no. 5, pp. 249–262, Oct. 2008.

[15] Z.-G. Wang, Z.-H. Liang, and C.-L. Liu, "A real-time image processor with combining dynamic contrast ratio enhancement and inverse gamma correction for PDP," *Displays*, vol. 30, no. 3, pp. 133–139, Jul. 2009.

[16] F.-C. Cheng and S.-J. Ruan, "Image quality analysis of a novel histogram equalization method for image contrast enhancement," *IEICE Trans. Inf. Syst.*, vol. E93-D, no. 7, pp. 1773–1779, Jul. 2010.

[17] T. Celik and T. Tjahjadi, "Contextual and variational contrast enhancement," *IEEE Trans. Image Process.*, vol. 20, no. 12, pp. 3431–3441, Dec. 2011.

[18] T. Celik and T. Tjahjadi, "Automatic image equalization and contrast enhancement using Gaussian mixture modeling," *IEEE Trans. Image Process.*, vol. 21, no. 1, pp. 145–156, Jan. 2012.

[19] M. Hanmandlu and D. Jha, "An optimal fuzzy system for color image enhancement," *IEEE Trans. Image Process.*, vol. 15, no. 10, pp. 2956–2966, Oct. 2006.

[20] M. Hanmandlu, O. P. Verma, N. K. Kumar, and M. Kulkarni, "A novel optimal fuzzy system for color image enhancement using bacterial foraging," *IEEE Trans. Instrum. Meas.*, vol. 58, no. 8, pp. 2867–2879, Aug. 2009.

[21] L. Zhang, L. Zhang, X. Mou, and D. Zhang, "FSIM: A feature similarity index for image quality assessment," *IEEE Trans. Image Process.*, vol. 20, no. 8, pp. 2378–2386, Aug. 2011.

[22] J.-K. Song and S. B. Park, "Rendering distortion assessment of image quality degraded by tone," *J. Disp. Technol.*, vol. 7, no. 7, pp. 365–372, Jul. 2011.

Shih-Chia Huang received the Doctorate degree in electrical engineering from National Taiwan University, Taipei, Taiwan, in 2009.

He is currently an Associate Professor with the Department of Electronic Engineering, National Taipei University of Technology, Taipei. He has authored or co-authored more than 20 papers in journals and conferences and holds more than 30 U.S. and Taiwan patents. His current research interests include image and video coding, wireless video transmission, video surveillance, error resilience and concealment techniques, digital signal processing, cloud computing, mobile applications and systems, embedded processor design, and embedded software and hardware co-design.

Prof. Huang was a recipient of the Kwoh-Ting Li Young Researcher Award from the Taipei Chapter of the Association for Computing Machinery in 2011.

Fan-Chieh Cheng received the Ph.D. degree in electronic engineering from the National Taiwan University of Science and Technology, Taipei, Taiwan.

He has authored or co-authored more than 10 articles in journals and conferences. His current research interests include digital image processing, video coding, and bus codec design, in particular, contrast enhancement, moving object detection, depth generation, super-resolution, motion estimation, and vehicular CAN bus transmission.

Yi-Sheng Chiu received the B.S. degree in electronic engineering from the National Chin-Yi University of Technology, Taichung, Taiwan, and the M.S. degree from the Department of Electronic Engineering, National Taipei University of Technology, Taipei, Taiwan, in 2007 and 2011, respectively.

His current research interests include video surveillance, contrast enhancement, and digital image and video processing.